Metal–Organic Frameworks

DOI: 10.1002/ange.201202471

A Water-Stable Porphyrin-Based Metal–Organic Framework Active for Visible-Light Photocatalysis**

*Alexandra Fateeva, Philip A. Chater, Christopher P. Ireland, Asif A. Tahir, Yaroslav Z. Khimyak, Paul V. Wiper, James R. Darwent, and Matthew J. Rosseinsky**

Metal–organic frameworks (MOFs) permit the combination of high internal surface area with chemical and physical functionality conferred by the molecular linker. Porphyrins are versatile functional molecules in catalysis,[1] light harvesting,[2] and molecular sensing.[3] Porphyrins have been used as building blocks for MOFs,[4] affording catalysts,[5] light harvesting[6] and selective sorption in liquid and gas phases.[7] MOFs based on Al-carboxylate coordination chemistry are amongst the most thermally and chemically stable of such systems reported to date.[8] Here we report a water-stable porous porphyrin MOF with a BET surface area of 1400 $m^2 g^{-1}$ which performs visible-light-driven hydrogen generation from water. The free-base porphyrin can be metalated within the rigid host structure.

The reaction of $AlCl_3 \cdot 6H_2O$ with the free-base *meso*-tetra(4-carboxyl-phenyl) porphyrin H_2TCPP (Figure 1b) in water under hydrothermal conditions at 180 °C followed by washing with dimethyl formamide (DMF) to remove unreacted ligand leads to the formation of the microcrystalline porous red compound $H_2TCPP[AlOH]_2(DMF_3(H_2O)_2)$ **1** (referred to as Al-PMOF, experimental details are given in section 1.1 in the Supporting Information). The linker consists of four benzoate groups around the central porphyrin core.[9] The analyzed composition reveals that no aluminium is coordinated within the porphyrin ring, consistent with the need to use reactive trialkylaluminium reagents for metalation of the porphyrin in solution.[10] The reaction temperature is required to solubilize the porphyrin linker. The crystal structure of **1** was solved and refined from synchrotron powder X-ray diffraction collected at 100 K. Indexing and Pawley refinement revealed an orthorhombic cell ($a = 31.978(3)$ Å, $b = 6.5812(4)$ Å, $c = 16.862(2)$ Å, $V = 3548.7(6)$ Å^3) consistent with the *C*222, *Cmm*2, and *Cmmm* space groups. Each of these candidate space groups was evaluated by simulated annealing using a semi-rigid body to describe the TCPP unit (Figure S1 in the Supporting Information) with eight refined parameters describing distances and angles within the porphyrin. The best results were obtained for the benzoic acid group perpendicular to the central porphyrin ring, which can be best described in *Cmmm* symmetry, and zero occupancy for Al at the center of the porphyrin. This model was used in the final Rietveld analysis (Figure 1a). Fourier mapping revealed a single guest atom in the channels attributed to oxygen from water, which was included in the final refinement (Figure S2 in the Supporting Information).

Each porphyrin linker in **1** is coordinated to eight aluminium centers (Figure 1c–e) through the four carboxylate groups which each bridge two aluminium units. There is

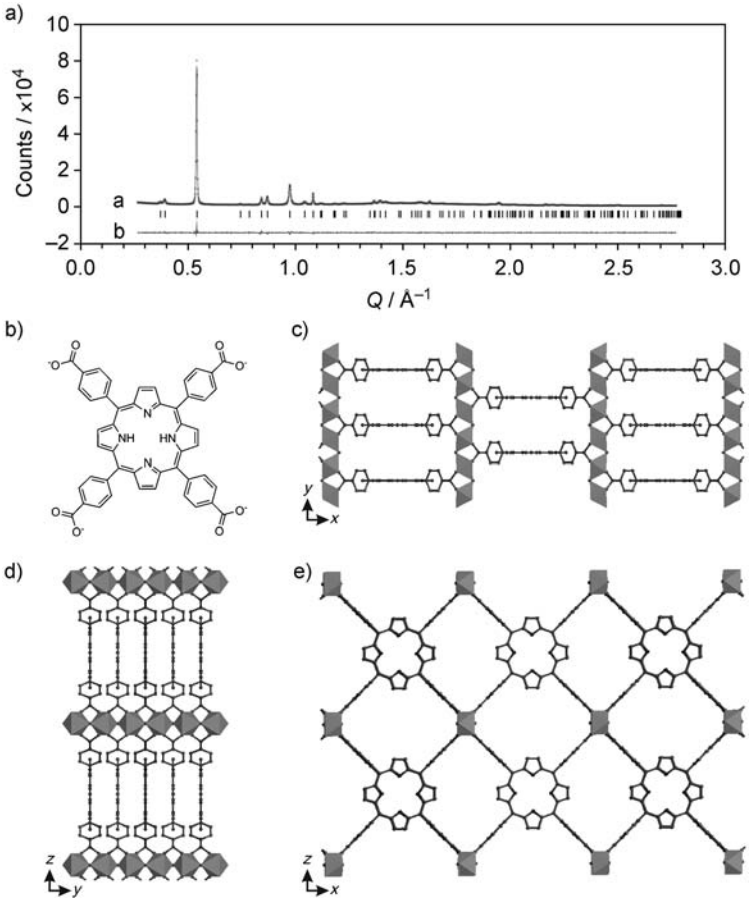

Figure 1. a) Final Rietveld refinement of **1** (100 K) showing observed (gray crosses), calculated (line a), and difference (line b) plots ($Q = 2\pi/d$). Bragg peak positions are indicated. b) TCPP porphyrinic linker in **1**. c–e) Crystal structure of **1** viewed down [001], [100], and [010] directions, respectively.

[*] Dr. A. Fateeva, Dr. P. A. Chater, C. P. Ireland, Dr. A. A. Tahir, Prof. Y. Z. Khimyak, P. V. Wiper, Prof. J. R. Darwent, Prof. M. J. Rosseinsky
Department of Chemistry, University of Liverpool
Liverpool, L697ZD (UK)
E-mail: m.j.rosseinsky@liv.ac.uk

[**] We thank the EPSRC for support under EP/H000925.
Supporting information for this article is available on the WWW under http://dx.doi.org/10.1002/anie.201202471.

a single, non-interpenetrated network defining the structure of **1**. The aluminium coordination consists of four carboxylate-derived oxygen atoms in the equatorial plane and two μ_2 axial OH^- bridging adjacent Al^{3+} centers to form an infinite $Al(OH)O_4$ chain, which is a common motif for M^{3+} frameworks with carboxylate ligands. The connectivity of **1** is comparable to MIL-60,[11] which is also based on a tetradentate ligand. Unlike MIL-60, the large, planar porphyrin unit arranges the chains into an almost perfectly square array. This arrangement of porphyrin linkers (equally spaced between pairs of $Al(OH)O_4$ chains, staggered in position along [010] between adjacent pairs of chains by their bridging coordination to Al which enforces tilting of the octahedra) produces an intricate, interlaced pore structure (Figure 2).

Two topologically distinct elliptical channels are present down the [010] direction; one with an in-plane arrangement of the porphyrin linkers giving rise to an hourglass-shaped pore (Figure 2b) and one with a staggered arrangement of the porphyrin linkers giving rise to an S-shaped pore (Figure 2d). Both elliptical pores are 6×11 Å (van der Waals radii subtracted) and are interconnected by smaller 5 Å rectangular pores running along [001] and [110] to give three-dimensional porosity (Figure 2c and e, respectively).

Consistent with the rigid porphyrin-based arrangement of the robust Al hydroxide chains, **1** is stable after guest loss to 350 °C in air (Figure S4 in the Supporting Information). Desolvation under vacuum (10^{-2} Pa) at 170 °C affords the guest-free material with both crystallinity and cell parameters essentially unchanged from the guest-containing system. N_2 sorption at 77 K demonstrates a surface area of 1400 m^2g^{-1} and a micropore volume of 0.625 cm^3g^{-1} which matches well with 0.63 cm^3g^{-1} calculated from the structural data at 100 K (Figure 2a).

Solid-state NMR spectroscopy confirms the structural chemistry deduced from the long-range average crystallographic structure of **1** at a local level. The ^1H magic angle spinning (MAS) NMR spectrum (Figure 3a) shows resonances at 9.0 and 7.8 ppm from the porphyrinic and benzyl rings, respectively, and −5.5 ppm from the NH protons of the free-base porphyrin linker. The resonance at 3.9 ppm is assigned to guest water species. The broad line at about 0 ppm is representative of bridging AlOHAl groups. The ^1H-^{13}C CP MAS NMR spectrum (Figure S6 in the Supporting Information) shows six resonances in the aromatic region corresponding to the carbon atoms of the porphyrin. The $^{27}Al\{^1H\}$ MAS NMR spectrum (Figure 3b) displays a broad, asymmetric resonance dominated by the second-order quadrupole interaction. The quadrupolar parameters (Table S2 in the Supporting Information) from lineshape fitting give an isotropic chemical shift at $\delta = 6.0$ ppm, a quadrupolar coupling constant of 13.5 MHz, and an asymmetry value of 0.13, indicating the presence of an octahedral AlO_6 site. These values are in agreement with Al-based porous frameworks containing similar structural units.[12] The ^{27}Al MQMAS NMR spectrum (Figure S7) confirms one AlO_6 site consistent with the predicted crystal structure.

The crystallinity of **1** is unchanged on standing for a week in water, with UV/Vis analysis of the supernatant confirming no porphyrin ligand is present in solution after this stability test. This stability extends to pH 5, with dissolution observed in both diffraction and UV/Vis spectroscopy at pH 8 and above (Figure 3c and d).

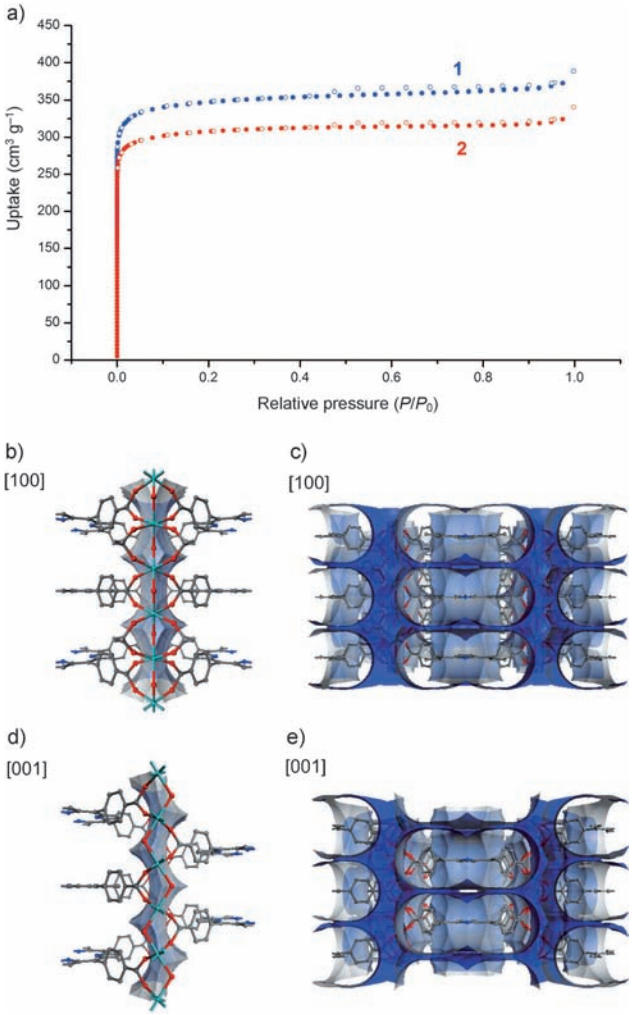

Figure 2. a) N_2 sorption isotherms at 77 K for **1** (blue) and **2** (red) upon adsorption (filled circles) and desorption (empty circles). b–e) Pore structure of **1**. The external and internal pore surfaces are shown in light gray and purple, respectively. b) Hourglass pore arising from the in-plane arrangement of porphyrin linkers, as probed by a radius of 1.8 Å. c) Section through the hourglass pore network, as probed by a radius of 1.4 Å. The hourglass pores are interconnected by smaller, rectangular channels in the [001] direction. d) S-shaped pore arising from the staggered arrangement of porphyrin linkers, as probed by a radii of 1.8 Å. e) Section though the hourglass pore network, as probed by a radii of 1.4 Å. The S-shaped pores are interconnected by smaller, rectangular channels in the [110] direction which in turn connect with the rectangular channels in the [001] direction to form a completely interconnected pore network.

The optical properties of **1** are determined by the porphyrin linker. The solid-state UV/Vis absorption spectra of the Al-PMOF shows the strong Soret band at 415 nm ($S_0\rightarrow S_2$ absorption process) and four Q bands at lower energies ($S_0\rightarrow S_1$), as expected from the π–π^* transitions in the free-base linker[13] (Figure 4a). The fluorescence spectrum (Figure 4b) displays a band at 660 nm arising from the $S_1\rightarrow S_0$

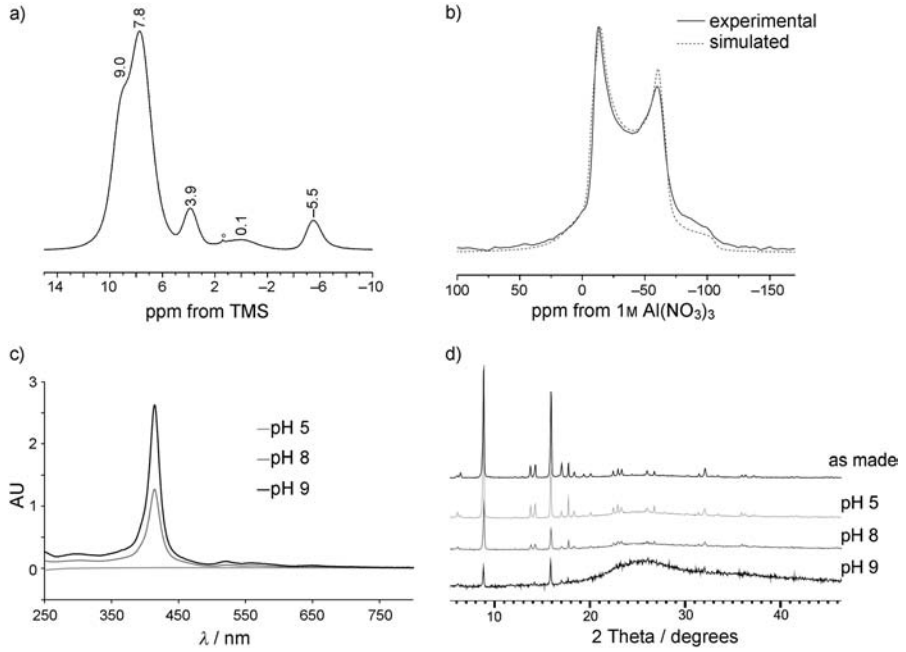

Figure 3. a–b) Solid-state NMR spectra of **1**: a) ^{1}H MAS at 25 kHz; b) ^{27}Al{^{1}H} MAS at 25 kHz. c) UV/Vis absorbance of the supernatant filtered from aqueous suspensions of **1** after standing for one week at ambient temperature at different pH. d) PXRD of solid **1** recovered after standing in aqueous solutions of varying pH.

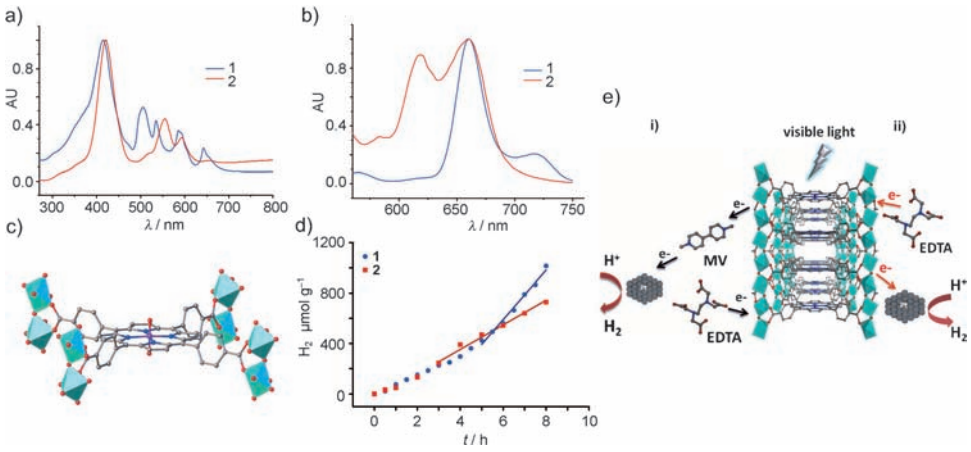

Figure 4. a) UV/Vis solid-state absorption spectra of **1** and **2**. b) Emission fluorescence spectra of **1** and **2** (excitation wavelength: 415 and 425 nm, respectively). c) Structure of the Zn^{2+}-metalated porphyrinic unit in **2**; Zn in purple. d) Photocatalytic evolution of hydrogen from water by **1** and **2** under visible-light illumination, using sacrificial EDTA with catalytic colloidal platinum e) The photocatalytic reaction using **2**. i) Reaction involving **2**, methyl viologen, colloidal platinum, and sacrificial EDTA. ii) Reaction involving **2**, colloidal platinum, and sacrificial EDTA. The relevant reaction equations are given in section S8.3 in the Supporting Information.

radiative processes, as expected for the free-base porphyrin and consistent with the spectrum of the free linker in solution (Figure S8 in the Supporting Information).

As the porphyrin is present in its free-base form, **1** can be considered as a versatile platform framework allowing post-synthetic chemical modification by porphyrin metalation. Reaction of **1** with anhydrous zinc acetate in DMF at 100 °C afforded a highly crystalline purple material **2** $Zn_{0.986(12)}$TCPP-$[AlOH]_2$ (see section 2 in the Supporting Information), consistent with 90 % occupancy of the porphyrin center sites by Zn^{2+} measured by energy dispersive X-ray spectroscopy (EDX) in conjunction with scanning electron microscopy (SEM). Material **2** refined with similar cell parameters to **1** (collected at 295 K, $a = 31.8577(14)$ Å, $b = 6.6002(3)$ Å, $c = 16.8909(8)$ Å, $V = 3551.6(3)$ Å^3). Rietveld refinement of synchrotron X-ray diffraction data from **2** desolvated at 443 K for 48 h under vacuum shows that Zn^{2+} is at the center of the porphyrin ring, with a refined occupancy of 0.986(12) in the plane of the porphyrin in square planar coordination (Figure 4c). Thermal stability measured by thermogravimetric analysis (TGA) increases over that of **1** to 370 °C (Figure S5) in air and the measured BET surface area is 1200 $m^2 g^{-1}$ (Figure 2a).

After metalation of the porphyrin ring to form **2**, the UV/Vis spectrum confirms Zn^{2+} insertion through a slight red shift in the Soret band to 425 nm (compared to 415 nm for **1**) and the predominant presence of two instead of four Q bands because of the higher symmetry of the metalated compound. The fluorescence spectrum also shows the effects of metalation on the optical properties, as the fluorescence signal of **2** displays two maxima at 620 and 660 nm, corresponding well to the effect of metalation on the ligand in solution (Figure S8 in the Supporting Information). Porphyrins have been evaluated for the photodissociation of water into H_2 and O_2.[2a,b,14] The photocatalytic properties of porphyrin molecules are sensitively controlled by the presence of metal cations within the ring.[15] As the porphyrin functionality is accessible through the extensive internal surface of **1** and **2**, and the porphyrin is photocatalytically active in visible light, we evaluated **1** and **2** for photocatalytic evolution of hydrogen from water. UV-absorbing MOFs have generated hydrogen from water photocatalytically[16] and recently Ir and Ru complex-doped UiO-67 proved to be catalytically active for organic transformations such as the aza-Henry reaction under

visible light.[17] To harvest the energy of the optically generated porphyrin-based excited states, two approaches were used. First the MOF/MV^{2+}/EDTA/Pt system was studied. Here the methyl viologen dication MV^{2+} acts as an electron acceptor and mediates electron transfer to Pt, which performs H_2 evolution and ethylenediaminetetracetic acid (EDTA) is a sacrificial electron donor (i in Figure 4e). MV^{2+} is readily adsorbed by **1** and **2** in an aqueous environment (Figure S9), and EDTA is far smaller than the available pore dimensions. Following absorption of visible light by the porphyrin and the generation of the associated electronic excited species in **1** or **2**, the methyl viologen is reduced to the radical cation ($MV^{+\bullet}$) by electron transfer from the porphyrin and EDTA is oxidized to organic decomposition products by the remaining positive charge on the porphyrin unit. $MV^{+\bullet}$ transfers its electron to the colloidal platinum where hydrogen is evolved. This reaction scheme is well-understood in the photochemistry of porphyrin molecules in solution (see section 8.3 in the Supporting Information). For both frameworks a small amount of H_2 was observed after illumination with visible light in the aqueous EDTA/MV^{2+}/colloidal Pt solution for 15 h (quantum yield estimated to be less than 0.01%). Such a low activity can be explained by the diffusion limitations of methyl viologen in the pores, as the Pt nanoparticles are too large to enter the pore system. To check this hypothesis, a second set of experiments was undertaken with the MOF/EDTA/Pt system. In this case the excited porphyrin molecules in the MOF react directly with EDTA to form the reduced porphyrin which in turn transfers an electron to Pt. Pt concentration was increased to ensure the optimum contact between the metal and the framework. For both frameworks there was a noticeable increase in H_2 generation, producing H_2 at 100 $\mu mol\,g^{-1}\,h^{-1}$ rate for **2** and 200 $\mu mol\,g^{-1}\,h^{-1}$ rate for **1** after an induction period of about 3 h, enhancing the quantum yield by more than one order of magnitude over the MV-based route (Figure 4d). Repeated reactions with same catalysts showed good data reproducibility. Powder X-ray diffraction (PXRD) and SEM measurements show that the frameworks are unchanged after the photocatalytic reactions (Figures S10, S11, and S12 in the Supporting Information). To rule out any homogeneous photocatalytic activity, a supernatant test was performed for **1** and **2**. After stirring the MOF in the reagent solution for 24 h, the solid was filtered out and the solution was exposed to visible-light source used for the photocatalysis reaction for 15 h. No H_2 could be detected by GC, showing that the amount of H_2 is produced by heterogeneous photocatalytic activity of the framework, consistent with the observed stability of **1** and **2** under the reaction conditions. We believe the low quantum yield is due to the self-quenching occurring inside the porphyrin MOFs **1** and **2**.

MOF **1** is a stable high-surface area crystalline material which presents the chemical and optical functionality of the porphyrin ligand for a range of applications. The center of the porphyrin ring is available for subsequent chemical modification in **1**, exploited here through the introduction of Zn^{2+}. More detailed control of the energy transfer processes following excitation of the porphyrin linker can be envisaged, for example, by diluting the concentration of porphyrin in the MOF or using alternative central metal ions in the porphyrin, to enhance the visible-light photocatalysis behavior observed.

Received: December 23, 2011
Revised: May 18, 2012
Published online: June 13, 2012

Keywords: heterogeneous catalysis · hydrogen production · metal–organic frameworks · porphyrinoids

[1] a) I. Bhugun, D. Lexa, J.-M. Savéant, *J. Phys. Chem.* **1996**, *100*, 19981–19985; b) H. Hennig, D. Luppa, *J. Prakt. Chem.* **1999**, *341*, 757–767; c) H. Sharghi, M. H. Beyzavi, M. M. Doroodmand, *Eur. J. Org. Chem.* **2008**, 4126–4138; d) H. Shinokubo, A. Osuka, *Chem. Commun.* **2009**, 1011–1021; e) M. Veyrat, O. Maury, F. Faverjon, D. E. Over, R. Ramasseul, J. C. Marchon, I. Turowskatyrk, W. R. Scheidt, *Angew. Chem.* **1994**, *106*, 200–203; *Angew. Chem. Int. Ed. Engl.* **1994**, *33*, 220–223.

[2] a) A. Harriman, *J. Chem. Soc. Faraday Trans. 1* **1981**, *77*, 369–377; b) A. Harriman, G. Porter, M.-C. Richoux, *J. Chem. Soc. Faraday Trans. 2* **1981**, *77*, 833–844; c) G. Knoer, A. Vogler, *Inorg. Chem.* **1994**, *33*, 314–318.

[3] a) C. Di Natale, D. Monti, R. Paolesse, *Mater. Today* **2010**, *13*, 37–43; b) I. Leray, M.-C. Vernières, C. Bied-Charreton, *Sens. Actuators A* **1999**, *54*, 243–251; c) S. Y. Tao, G. T. Li, *Colloid Polym. Sci.* **2007**, *285*, 721–728; d) Y. S. Xie, J. P. Hill, R. Charvet, K. Ariga, *J. Nanosci. Nanotechnol.* **2007**, *7*, 2969–2993.

[4] a) P. M. Barron, H. T. Son, C. H. Hu, W. Choe, *Cryst. Growth Des.* **2009**, *9*, 1960–1965; b) P. M. Barron, C. A. Wray, C. H. Hu, Z. Y. Guo, W. Choe, *Inorg. Chem.* **2010**, *49*, 10217–10219; c) P. Bhyrappa, S. R. Wilson, K. S. Suslick, *J. Am. Chem. Soc.* **1997**, *119*, 8492–8502; d) B. J. Burnett, P. M. Barron, C. Hu, W. Choe, *J. Am. Chem. Soc.* **2011**, *133*, 9984–9987; e) E. Y. Choi, P. M. Barron, R. W. Novotney, C. H. Hu, Y. U. Kwon, W. Y. Choe, *CrystEngComm* **2008**, *10*, 824–826; f) E. Y. Choi, P. M. Barron, R. W. Novotny, H. T. Son, C. H. Hu, W. Choe, *Inorg. Chem.* **2009**, *48*, 426–428; g) H. Chung, P. M. Barron, R. W. Novotny, H. T. Son, C. Hu, W. Choe, *Cryst. Growth Des.* **2009**, *9*, 3327–3332; h) L. D. DeVries, P. M. Barron, E. P. Hurley, C. H. Hu, W. Choe, *J. Am. Chem. Soc.* **2011**, *133*, 14848–14851; i) M. E. Kosal, J. H. Chou, K. S. Suslick, *J. Porphyrins Phthalocyanines* **2002**, *6*, 377–381; j) M. E. Kosal, K. S. Suslick, *J. Solid State Chem.* **2000**, *152*, 87–98; k) S. Lipstman, I. Goldberg, *CrystEngComm* **2010**, *12*, 52–54; l) S. Lipstman, S. Muniappan, S. George, I. Goldberg, *Dalton Trans.* **2007**, 3273–3281; m) S. Lipstman, S. Muniappan, I. Goldberg, *Acta Crystallogr. Sect. C* **2007**, *63*, O371–O373; n) K. S. Suslick, N. A. Rakow, M. E. Kosal, J. H. Chou, *J. Porphyrins Phthalocyanines* **2000**, *4*, 407–413; o) B. F. Abrahams, B. F. Hoskins, D. M. Michail, R. Robson, *Nature* **1994**, *369*, 727–729.

[5] a) C. N. Kato, M. Ono, T. Hino, T. Ohmura, W. Mori, *Catal. Commun.* **2006**, *7*, 673–677; b) T. Sato, W. Mori, C. N. Kato, E. Yanaoka, T. Kuribayashi, R. Ohtera, Y. Shiraishi, *J. Catal.* **2005**, *232*, 186–198; c) A. M. Shultz, O. K. Farha, J. T. Hupp, S. T. Nguyen, *J. Am. Chem. Soc.* **2009**, *131*, 4204–4205.

[6] C. Y. Lee, O. K. Farha, B. J. Hong, A. A. Sarjeant, S. T. Nguyen, J. T. Hupp, *J. Am. Chem. Soc.* **2011**, *133*, 15858–15861.

[7] a) A. Fateeva, S. Devautour-Vinot, N. Heymans, T. Devic, J.-M. Grenèche, S. Wuttke, S. Miller, A. Lago, C. Serre, G. De Weireld, G. Maurin, A. Vimont, G. Férey, *Chem. Mater.* **2011**, *23*, 4641–4651; b) M. E. Kosal, J. H. Chou, S. R. Wilson, K. S. Suslick, *Nat. Mater.* **2002**, *1*, 118–121; c) D. W. Smithenry, S. R. Wilson, K. S. Suslick, *Inorg. Chem.* **2003**, *42*, 7719–7721.

[8] a) I. J. Kang, N. A. Khan, E. Haque, S. H. Jhung, *Chem. Eur. J.* **2011**, *17*, 6437–6442; b) J. J. Low, A. I. Benin, P. Jakubczak, J. F.

Abrahamian, S. A. Faheem, R. R. Willis, *J. Am. Chem. Soc.* **2009**, *131*, 15834 – 15842.
[9] P. Dastidar, Z. Stein, I. Goldberg, C. E. Strouse, *Supramol. Chem.* **1996**, *7*, 257 – 270.
[10] a) T. Aida, S. Inoue, *J. Am. Chem. Soc.* **1983**, *105*, 1304 – 1309; b) S. Asano, T. Aida, S. Inoue, *Macromolecules* **1985**, *18*, 2057 – 2061.
[11] K. Barthelet, D. Riou, M. Nogues, G. Férey, *Inorg. Chem.* **2003**, *42*, 1739 – 1743.
[12] a) T. Loiseau, C. Serre, C. Huguenard, G. Fink, F. Taulelle, M. Henry, T. Bataille, G. Férey, *Chem. Eur. J.* **2004**, *10*, 1373 – 1382; b) C. Volkringer, T. Loiseau, N. Guillou, G. Férey, M. Haouas, F. Taulelle, E. Elkaim, N. Stock, *Inorg. Chem.* **2010**, *49*, 9852 – 9862.
[13] D. Marsh, L. Mink, *J. Chem. Educ.* **1996**, *73*, 1188.
[14] J. R. Darwent, P. Douglas, A. Harriman, G. Porter, M. C. Richoux, *Coord. Chem. Rev.* **1982**, *44*, 83 – 126.
[15] a) B. A. Jean, S. B. Ralph, *J. Chem. Phys.* **1960**, *32*, 1410 – 1417.
[16] C. Gomes Silva, I. Luz, F. X. Llabrés i Xamena, A. Corma, H. García, *Chem. Eur. J.* **2010**, *16*, 11133 – 11138.
[17] C. Wang, Z. Xie, K. E. deKrafft, W. Lin, *J. Am. Chem. Soc.* **2011**, *133*, 13445 – 13454.